PROCEEDINGS OF SCIENCE

Particle acceleration in a relativistic shock in inhomogeneous media

Kanji Morikawa[a,*] **and Yutaka Ohira**[a]

[a] *Department of Earth and Planetary Science, The University of Tokyo, 7-3-1 Hongo, Bunkyo-ku, Tokyo, 113-0033 Japan*

E-mail: kanji.m1029@eps.s.u-tokyo.ac.jp, y.ohira@eps.s.u-tokyo.ac.jp

It is known that the maximum energy of Cosmic Rays (CRs) reaches to 10^{20} eV. One of the candidates of the acceleration mechanism of these highest-energy CRs is shock acceleration in a relativistic shock. However, it is also known that in a relativistic shock, particles cannot go back and forth around the shock many times, because there is almost no difference between the shock velocity and the particle velocity. In this work, we consider density fluctuations in the shock upstream region. The interaction of density fluctuations and a relativistic shock drives the turbulence in the shock downstream region. This turbulence could change their direction of particle motion. We carried out the MagnetoHydroDynamic (MHD) simulations and test-particle simulations to check this mechanism can accelerate the CRs. We found that particles can cross the shock front many times thanks to scattering by the downstream region. In addition, the amplitude of the density fluctuation is an important parameter to determine the acceleration efficiency. We revealed a condition where particles can cross the shock many times.

38th International Cosmic Ray Conference (ICRC2023)
26 July - 3 August, 2023
Nagoya, Japan

ICRC2023
38th International Cosmic Ray Conference
The Astroparticle Physics Conference

*Speaker

PoS(ICRC2023)378

1. Introduction

It is proposed that Ultra-High-Energy Cosmic Rays (UHECRs) are accelerated by Diffusive Shock Acceleration (DSA) mechanism or First-order Fermi acceleration mechanism in a relativistic shock. For example, Gamma-Ray Bursts (GRB) or Active Galactic Nuclei (AGN) have relativistic shocks. However, it is known that particles cannot be accelerated efficiently in a relativistic shock propagating in a uniform magnetic field and they cannot reach the energy of 10^{20} eV [7]. This is because the bulk velocity downstream is so high that the particles are drifted to far downstream rapidly.

It is also known that even in a relativistic shock, particles can cross the shock many times by scattering due to some turbulence [8]. For example, Weibel-mediated shock can generate some turbulence in a relativistic shock. By the Weibel turbulence, particles are scattered and cross the shock front, but the acceleration time scale is too long to accelerate CR to the UHECRs energy scale [10]. Thus, we cannot explain the origin of UHECRs in a relativistic shock by the turbulence due to Weibel-mediated shock.

In this work, we focus on density fluctuations in the upstream region. When a relativistic shock propagates in a nonuniform medium, the interaction between the density fluctuations and the shock drives turbulence in the downstream region. In a non-relativistic shock, such as a supernova remnant, this mechanism works and the magnetic field is amplified in the downstream region, but in the case of a relativistic shock, no one knows if this works efficiently [5, 6]. Furthermore, this mechanism works less efficiently in a relativistic shock [11]. We investigate the amplification of the magnetic field in a relativistic shock, and whether it can accelerate particles or not.

2. Simulations

2.1 Three-dimensional relativistic MHD simulations

The electromagnetic field in the downstream region is important for particles to be scattered and return to the upstream region. We performed 3D relativistic MagnetoHydroDynamic (MHD) simulations in order to obtain the downstream field. We used the MHD simulation code called SRCANS+ developed by Y. Matsumoto (Chiba Univ.) and T. Ohmura (ICRR). The box size is 8000 grids in the x direction, and 200 grids in the y and z directions, respectively.

We calculated the MHD simulation in the shock rest frame. Thus, we can calculate the test-particle simulation by using the results of MHD simulations as a snapshot data. Note that the upstream density fluctuation is compressed by the Lorentz factor of the shock wave in the shock rest frame by Lorentz contraction. The downstream turbulence is dissipated eventually. The relation between the time scale of turbulent evolution $t_{\rm eddy}$ and the time scale of turbulent decay $t_{\rm dec}$ is given by [11]

$$t_{\rm dec} = \frac{n_{\rm cl}}{\Gamma n} t_{\rm eddy},$$

where $\Gamma, n, n_{\rm cl}$ is the Lorentz factor of the shock, uniform number density in the upstream region, and clump density in the clump rest frame. In this study, we investigate dependence of the amplitude of the density fluctuation, $\delta n_{\rm cl}/n = 1$ and $\delta n_{\rm cl}/n = 10$.

The distribution of the number density around each clump is given by

$$n(x,y) = \begin{cases} n_0 & (r > 2R_{\rm cl}) \\ n_0 + (n_{\rm cl} - n_0)\left\{1 + \cos\left(\frac{\pi r}{2R_{cl}}\right)\right\} & (r \leqq 2R_{\rm cl}) \end{cases},$$

$$r \equiv \sqrt{\frac{(x-x_{\rm c})^2}{\Gamma^2} + (y-y_{\rm c})^2 + (z-z_{\rm c})^2},$$

where n_0 and Γ are the background number density and the bulk Lorentz factor. $x_{\rm c}, y_{\rm c}, z_{\rm c}$ is the center of each density clump. For simplicity, we assume that the shape of these clumps is spherical and all clumps have the same size in the upstream rest frame. We randomly distribute many clumps in the upstream region.

We assume that the bulk flow is in the x direction and the initial magnetic field is parallel to the y direction in the simulations.

2.2 Test-particle simulations

Next, we calculated test-particle simulations using the electromagnetic field obtained by the MHD simulations. The test-particle simulations are calculated in the shock rest frame. We approximately use the snapshot field data. This is valid because downstream velocity fluctuations are sufficiently smaller than the velocity of the test particles. We solved the equation of motion of relativistic particles. The time step Δt in the simulation is given by

$$\Delta t = \frac{1}{100} T_{\rm up}.$$

We randomly inject test particles in the far upstream region. All particles initially have the same four velocity of $u_r = 10$ in the upstream rest frame. Moreover, their direction is isotropic in the upstream rest frame. The number of test particles is 10^7 for each simulation. The free parameter is the ratio of the gyro radius of the particles to the size of the density fluctuation.

3. Results

3.1 Three-dimensional MHD simulations

First, we show the results of the MHD simulations. Figure 1 shows the snapshot of the magnetic field and density in x-y and x-z plane for the case of $\delta n_{\rm cl}/n = 1$. Figure 2 is the same as Figure 1, but for the case of $\delta n_{\rm cl}/n = 10$. The shock front is located around $x = 4800$.

3.2 Test-Particle simulations

Next, we show the results of the test-particle simulations. In the test-particle simulations, we used snapshot data from the MHD simulation, which is no temporal variation. The parameter is the ratio of gyro radius upstream to the size of the magnetic structure. We performed two simulations by changing the ratio of gyro radius of injected particles $r_{\rm gyro,up}$ to the size of density fluctuation, $\lambda = 0.1 L_{\rm y}$, where $L_{\rm y}$ is the size of the simulation box in y direction. Table 1 shows the summary of test-particle simulation results.

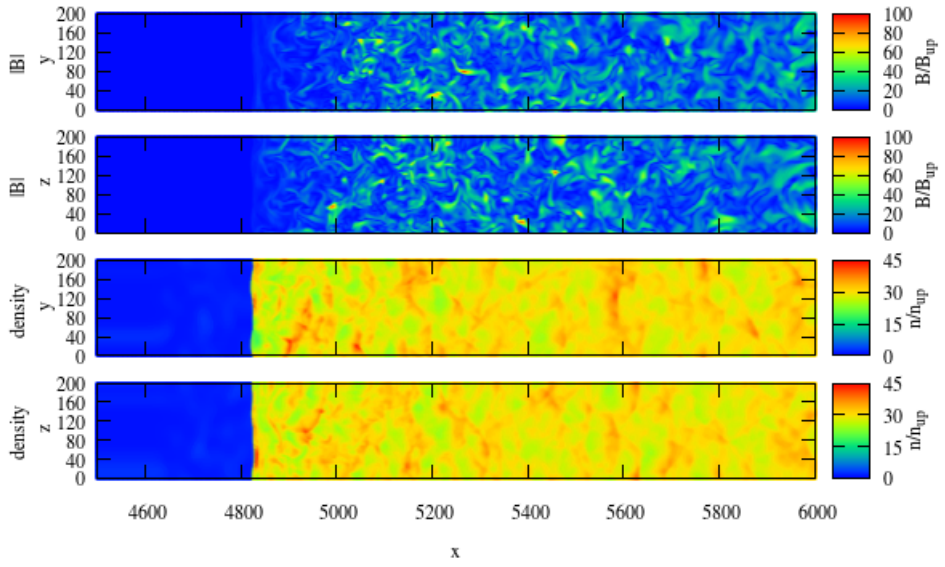

Figure 1: The magnetic field strength, $|B|$, and density distributions in the x-y and x-z planes for $\delta n_{\rm cl}/n = 1$.

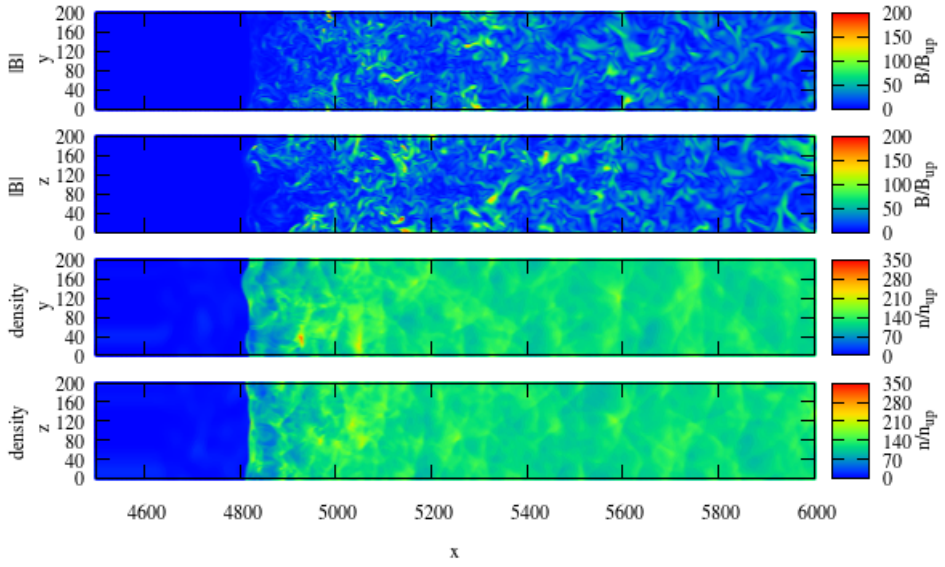

Figure 2: The same as Figure 1, but for $\delta n_{\rm cl}/n = 10$.

Figure 3 shows the energy spectra for $r_{\rm gyro,up} = 10\lambda$. We can see that particles are efficiently accelerated to higher energy for $\delta n_{\rm cl}/n = 10$.

Finally, we show the time evolution of the highest energy particle in the simulation for the case of $\delta n_{\rm cl}/n = 10$ and $r_{\rm gyro,up} = 10\lambda$ in Figure 4. As one can see, the particle can go back to the upstream region several times. Since the upstream region has an uniform magnetic field and convective electric field in the shock rest frame (simulation frame), particles in the upstream region

	$\delta n_{\rm cl}/n = 1$	$\delta n_{\rm cl}/n = 10$
$r_{\rm gyro,up} = \lambda$	not accelerated	mildly accelerated
$r_{\rm gyro,up} = 10\lambda$	mildly accelerated	accelerated

Table 1: Summary of test-particle simulations.

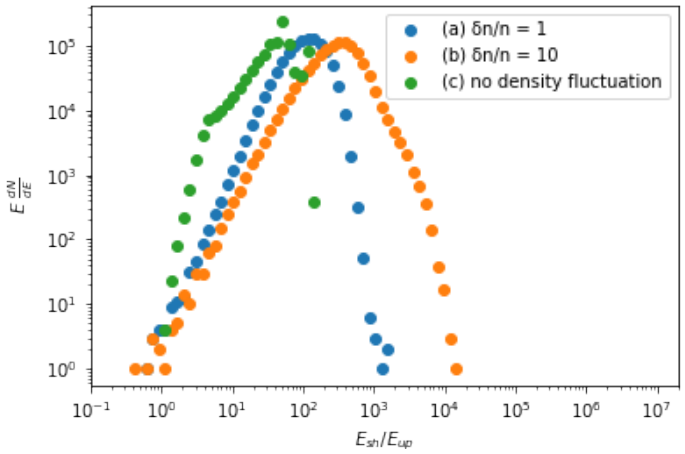

Figure 3: Energy spectra of test-particle simulations for $r_{\rm gyro,up} = 10\lambda$. The horizontal axis shows the final particle energy in the shock rest frame, which is normalized by the initial particle energy in the shock rest frame, $E_{\rm up}$. The orange, blue, and green points show energy spectra for $\delta n_{\rm cl}/n = 10$, $\delta n_{\rm cl}/n = 1$, and $\delta n_{\rm cl}/n = 0$, respectively.

are advected to the downstream region eventially. On the other hand, in the downstream region, particles are scattered by turbulent magnetic fields.

4. Discussion

We found that particles can be accelerated by First-order Fermi acceleration mechanism in a relativistic shock propagating in an inhomogeneous medium. In such a situation, turbulence is generated around the shock front in downstream, and this makes the particles go back to the upstream region. This is because the magnetic field is amplified downstream at a smaller distance than the gyro radius of the particles from the shock front, resulting in a significant change in the trajectory of the particles. We need to investigate in more detail how the turbulence near the shock front evolves with respect to the gyro radius of the particles. In our test-particle simulations, the results of the MHD simulations were used only up to x = 6000 due to the computational resources. Since the particles gain energy with each round trip of the shock front and the gyro radius increases, the box size limits the maximum energy in our simulations. This problem will be solved with further computational resources.

In Figure 3, the peak energy is shifted to a higher energy as the density fluctuations are large.

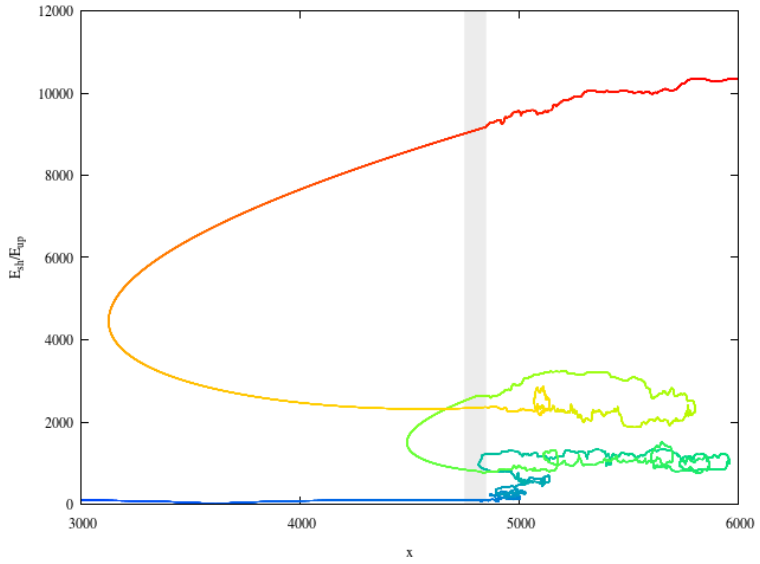

Figure 4: Trajectory of the most energetic particle in the test-particle simulation. The gray region around $x = 4800$ shows the mean shock potion averaged over y and z direction. The color of this trajectory means the time evolution of the particle trajectory. As the particle crosses the shock front several times, it gain energy.

This might be due to Second-order Fermi acceleration caused by turbulence in the downstream region.

acknowledgement

acNumerical computations were carried out on Cray XC50 at Center for Computational Astrophysics (CfCA), National Astronomical Observatory of Japan. K. M. is supported by International Graduate Program for Excellence in Earth-Space Science (IGPEES), The University of Tokyo. Y. O. is supported by JSPS KAKENHI Grants No. JP19H01893 and No. JP21H04487. In addition, we would like to thank Prof. Matsumoto from Chiba Univ. and Dr. Ohmura from ICRR who developed the 3D relativistic simulation code, SRCANS+.

References

[1] A. Achterberg, Y. A. Gallant, J. G. Kirk, and A. W. Guthmann. Particle acceleration by ultrarelativistic shocks: theory and simulations. *Monthly Notices of the Royal Astronomical Society*, 328(2):393–408, 12 2001.

[2] A. R. Bell. The acceleration of cosmic rays in shock fronts – I. *Monthly Notices of the Royal Astronomical Society*, 182(2):147–156, 02 1978.

[3] R. D. Blandford and J. P. Ostriker. Particle acceleration by astrophysical shocks. *Astrophysical Journal Letters*, 221:L29–L32, 1978.

[4] J. Giacalone and J. R. Jokipii. Charged-particle motion in multidimensional magnetic-field turbulence. *The Astrophysical Journal Letters*, 430(2):L137, aug 1994.

[5] Y. Hu, S. Xu, J. M. Stone, and A. Lazarian. Turbulent magnetic field amplification by the interaction of a shock wave and inhomogeneous medium. *The Astrophysical Journal*, 941(2):133, dec 2022.

[6] T. Inoue, K. Asano, and K. Ioka. Three-dimensional simulations of magnetohydrodynamic turbulence behind relativistic shock waves and their implications for gamma-ray bursts. *The Astrophysical Journal*, 734(2):77, may 2011.

[7] M. Lemoine, G. Pelletier, and B. Revenu. On the efficiency of fermi acceleration at relativistic shocks. *The Astrophysical Journal*, 645(2):L129, jul 2006.

[8] M. Lemoine and B. Revenu. Relativistic Fermi acceleration with shock compressed turbulence. *Monthly Notices of the Royal Astronomical Society*, 366(2):635–644, 02 2006.

[9] J. Niemiec, M. Ostrowski, and M. Pohl. Cosmic-ray acceleration at ultrarelativistic shock waves: Effects of downstream short-wave turbulence. *The Astrophysical Journal*, 650(2):1020, 2006.

[10] L. Sironi, A. Spitkovsky, and J. Arons. The maximum energy of accelerated particles in relativistic collisionless shocks. *The Astrophysical Journal*, 771(1):54, jun 2013.

[11] S. Tomita, Y. Ohira, S. S. Kimura, K. Tomida, and K. Toma. Interaction of a relativistic magnetized collisionless shock with a dense clump. *The Astrophysical Journal Letters*, 936(1):L9, aug 2022.